Glycoconj J (2006) 23:355–369
DOI 10.1007/s10719-006-8492-3

Distinctive characteristics of MALDI-Q/TOF and TOF/TOF tandem mass spectrometry for sequencing of permethylated complex type N-glycans*

Shin-Yi Yu[#] · Sz-Wei Wu[#] · Kay-Hooi Khoo

Received: 26 October 2005 / Revised: 2 January 2006 / Accepted: 5 January 2006

Abstract Concerted MALDI-MS profiling and CID MS/MS sequencing of permethylated glycans is one of the most effective approaches for high throughput glycomics applications. In essence, the identification of larger complex type N-glycans necessitates an unambiguous definition of any modification on the trimannosyl core and the complement of non-reducing terminal sequences which constitute the respective antennary structures. Permethylation not only affords analyses of both neutral and sialylated glycans at comparable ease and sensitivity but also yields more sequence-informative fragmentation pattern. Facile glycosidic cleavages directed mostly at *N*-acetylglucosamine under low energy CID, as implemented on a quadrupole/time-of-flight (Q/TOF) instrument, often afford multiple losses of the attached antenna resulting in characteristic ions related to the number of antennary branches on the trimannosyl core. Non-reducing terminal epitopes can be easily deduced but information on the linkage specific substituent on the terminal units is often missing. The high energy CID MS/MS afforded by TOF/TOF instrument can fill in the gap by giving an array of additional cross-ring and satellite ions. Glycosidic cleavages occurring specifically in concert with loss of 2-linked or 3-linked substituents provide an effective way to identify the branch-specific antennary extension. These characteristics are shown here to be effective in deriving the sequences of additionally galactosylated, sialylated and fucosylated terminal *N*-acetyllactosamine units and their antennary location. Together, a highly reproducible fragmentation pattern can be formulated to simplify spectral assignment. This work also provides first real examples of sequencing multiply sialylated complex type N-glycans by high energy CID on a TOF/TOF instrument.

Keywords Glycan sequencing · High energy CID MS/MS · MALDI TOF/TOF · Mass spectrometry

Abbreviations

CID	collision-induced dissociation
EI	electron impact
ESI	electrospray ionization
FAB	fast atom bombardment
MALDI	matrix assisted laser desorption/ionization
MS	mass spectrometry
MS/MS	tandem mass spectrometry
Q/TOF	quadrupole/time-of-flight
LacNAc	*N*-aectyllactosamine
OMe	O-methyl substituent or methoxy

Introduction

High throughput and robust MALDI-based mass spectrometry (MS) profiling is often the preferred, principal "first screen" strategy in defining the complexity and characteristics of a glycome [1]. In comparison with ESI-based MS analysis, the singly charged nature of the afforded molecular ions gives an added advantage in spectral simplicity and thus the ease of interpretation of a highly heterogeneous glycosylation profile. From a perspective of glycomic

[#]Shin-Yi Yu and Sz-Wei Wu contributed equally to this work.

*Dedicated to the late Prof. Yasuo Inoue, without whom the body of work represented by this article would not have been initiated in Taiwan.

S.-Y. Yu · S.-W. Wu · K.-H. Khoo (✉)
Institute of Biological Chemistry, Academia Sinica, Taiwan
e-mail: kkhoo@gate.sinica.edu.tw
Tel: 886-2-2785-5696
Fax: 886-2-2788-2043

K.-H. Khoo
National Core Facilities for Proteomics Research,
Academia Sinica, Taiwan

analysis, capability to subsequently perform high quality collision-induced dissociation (CID) MS/MS analyses directly on selected peaks is a requisite to critically define the ensemble of non-reducing terminal epitopes and core types among a myriad of isobaric glycan signals. Arguably, such an offline approach in targeted MALDI MS/MS analysis would be preferable to one that is constrained by the time scale of an online LC-ESI-MS/MS analysis which is difficult to incorporate an intelligent data dependent acquisition logic other than that defined by parent ion intensity.

MS analysis of permethyl derivatives dated back almost as early as the history of carbohydrate analysis. It was first implemented out of necessity for EI- and then FAB-ionization sources. Fragmentation pattern was carefully examined and a body of historical work [2–5] has provided a firm mechanistic basis for much of our current day understanding. The fundamental differences in the specific cleavages afforded by protonated versus other cationized parent ions, or low (<100 eV) *versus* high (up to several keV) collision energy, or different collision gases, were noted then for FAB CID-MS/MS, as carried out on either a triple quadrupole or a four sector instrument [5]. The advent of ESI in the 90s has since led to many MS/MS studies along the line of low energy CID [6–12] and an important trend has been to apply the analysis directly on underivatized glycan samples [13–20], or one that has been tagged at the reducing end [21–28] primarily to facilitate coupling to liquid chromatography. Although subsequent nanoESI and MALDI sources have practically overcome the sensitivity problem of analyzing native glycans, many advantages remain with analysis of permethyl derivatives, especially in sequencing real biological samples of unknown structures [29].

Permethylation often provides a simple way of cleaning up the glycan samples from its biological buffers, by imparting them hydrophobic nature and thus conducive to reverse phase type of purification. Further sample pre-treatment before MS analysis is usually less critical and spectra of better quality can usually be obtained with apparent enhancement of signal to noise ratio per same amount of sample applied. This is as true for MALDI as is for ESI. Secondly, and perhaps more importantly, is the conversion of sialic acid to methyl ester and thus neutralize the multiple negative charges carried by sialylated glycans. This stabilizes the sialic acid residues which would otherwise prone to loss from the native glycans during MS analysis and cannot be differentiated from genuine structures with lower degree or no sialylation. A third advantage resides in a more predictable fragmentation characteristic which is also easier to interpret with much less ambiguity.

Efficient MALDI CID-MS/MS is made possible by recent advances in MS instrumentation, first with coupling of MALDI source to a Q/TOF [30,31] and later to TOF/TOF [32], both of which rapidly superseded MALDI MS/MS in post-source decay (PSD) mode [33,34]. Systematic investigation of the low energy CID fragmentation characteristics as implemented on a MALDI Q/TOF is thus far restricted to native glycans [30] or those tagged at reducing end [35] although it is recognized from several applications [36,37] that the fragmentation pattern afforded by the permethyl derivatives is similar to that given by ESI CID-MS/MS on the Q/TOF [11,38] or the ion traps [7–10], which have been extensively studied. In general for larger N-glycans, the lack of linkage-specific cross-ring cleavages coupled with the predominant glycosidic cleavages have significantly limited its ability to provide fine sequence details. Several efforts are now channeled towards intelligent implementation of multistage MS/MS (MS^n), exploiting the recent generation of ion traps of higher capacity, faster scan rate and ultimately higher sensitivity [12,28,39,40]. Multistage analysis is particularly needed to extract more linkage-specific information from what can be provided by a single first stage MS/MS (MS^2) spectrum afforded by an ion trap.

As an alternative to low energy CID MS^n approach on ion traps which is mostly restricted to ESI, it is clear from earlier studies [5], that a single stage, MALDI-based, high energy CID MS/MS will provide highly complementary sequencing data, complete with linkage information. A first insight was provided by a seminal study on the MALDI high energy CID-MS/MS of native glycans as performed on a hybrid sector-orthogonal TOF instrument [41]. Three classes of fragment ions were distinguished *i.e.* the glycosidic, cross-ring, and internal double cleavage ions, where linkage information was mainly derived from the latter two types of ions, as would be expected. The subsequent commercialization and gaining in popularity of TOF/TOF MS instruments has led to several more recent investigations into the afforded high energy CID fragmentation pattern of both native [42,43] and permethylated [44,45] glycans, each reporting specific sets of cleavages that are linkage-specific. In essence, although the proposed mechanism for their formation may vary and in most cases without experimental evidence, the actual product ions afforded by high energy CID MS/MS on the current TOF/TOF instruments appear to share the same characteristics. There is clearly a need to assimilate all disparate observation into sets of rules that can be used not only to guide manual *de novo* sequencing but also for future formulation into algorithms governing auto-sequencing application software in tune with glycomics. In addition, apart from one study conducted on permethyl derivatives of several milk oligosaccharides of 3-6 residues [45], none of the other MALDI-based high energy CID MS/MS studies [41–44] have examined sialylated glycans.

We propose here, short of using multistage MS^n, *de novo* sequencing of complex type N-glycans is most readily accomplished by complementary low and high energy CID MS/MS on their permethyl derivatives. Using representative application examples from a diverse collection of samples

analyzed, we demonstrate in this report how various cleavage ions can be readily identified and the particular information they carry. Notably, we report on the fragmentation characteristics of a variety of commonly found non-reducing terminal epitopes such as the α-galactosylated, α-fucosylated, and/or sialylated *N*-aectyllactosmine (LacNAc) units, as carried on complex type *N*-glycans. We further show that the features established can be used to sequence several novel structures and, in the process, confirm their linkages and sequences, as defined elsewhere by more conventional approaches. Multiply sialylated multiantennary N-glycans including those with disialylated antennae can likewise be analyzed at comparable ease and sequence-assigned accordingly.

Materials and methods

N-Glycan samples

The asialo triantennary complex type N-glycan was purchased from Calbiochem. Trifucosylated triantennary N-glycan was kindly provided by Dr. Chun-Hung Lin, IBC, Academia Sinica, by treating the standard with recombinant α1,3-fucosyltransferase from *H. pylori*, in a reaction buffer containing 100 mM Tris-HCL, 1 mM $MnCl_2$, and 1 mM GDP-Fuc. Core fucosylated tetraantennary N-glycans were obtained from recombinant erythropoietin expressed in BHK cells. α3-Galactosylated bi-, and triantennary, core fucosylated N-glycans originated from glycoprotein extracts of rabbit erythrocytes (source provided by Dr. Gary Clark, University of Missouri School of Medicine; N-glycopeptides prepared by Dr. Mark Sutton-Smith, Imperial College, UK). The sample was further treated with α-galactosidase to remove the terminal α3-Gal. Detailed characterization of the α-galactosylated N-glycans is reported elsewhere. The bisected biantennary N-glycans comprising differentially fucosylated isomers were selected from the glycomic profiling of a colonic adenocarcinoma cell line, Colo205. Tri- and tetrasialylated triantennary N-glycans were released from tryptic peptides of fetuin (from fetal bovine serum, Sigma) by PNGase F using a standard protocol as described previously [36]. Trisialylated biantennary N-glycans from sera of mice implanted with murine tumor was prepared and provided by Dr. Shu-Yu Lin (Core Facilities for Proteomics Research, Academia Sinica). N-glycans from zebrafish embryos were prepared, structurally characterized and reported in detail elsewhere [46]. All glycan samples were permethylated using the NaOH/dimethyl sulfoxide slurry method [47] as described by Dell *et al.* [48]. The permethyl derivatives were then extracted in chloroform and repeatedly washed with water.

MS and MS/MS analysis

MALDI-MS/MS sequencing of permethylated N-glycans were performed on either a Q-TOF Ultima^{TM} MALDI (Micromass, Manchester, UK) or a 4700 Proteomics Analyzer (Applied Biosystems, Framingham, MA), both operated in reflectron positive ion mode. For acquisition on Q-TOF, the permethylated samples in acetonitrile were mixed 1:1 with α-cyano-4-hydrocinnamic acid matrix (5 mg/ml in 50% acetonitrile/0.1% trifluoroacetic acid) for spotting onto the target plate. MS survey and CID MS/MS data were manually acquired. Argon was used as the collision gas with a collision energy manually adjusted (between 100 $\sim$ 200 V) to achieve optimum degree of fragmentation for the parent ions under investigation.

Data acquisition on the TOF/TOF instrument was performed using the 2,5-dihydroxybenzoic acid (DHB) matrix (10 mg/ml in water, mixed 1:1 with sample dissolved in acetonitrile). MS survey data were acquired either with automated or manual target plate movement depending on state of crystallization. A typical data acquisition comprises a total of 20 sub-spectra of 125 laser shots each with laser energy normally set at 4500. CID MS/MS data were acquired manually, typically comprise a total of 40 sub-spectra of 125 laser shots at a laser energy setting of 5300-5800, but can be varied depending on the intensity of parent ion. Two or more spectra can be combined post-acquisition with mass tolerance set at 0.1 Da to improve S/N ratio. The potential difference between the source acceleration voltage and the collision cell was set at 2 kV to obtain the desirable high energy CID fragmentation pattern. The indicated collision cell pressure was normally increased from 3.0×10^{-8} torr (no collision gas) to 5.0×10^{-7} torr (argon).

Results and discussion

Fragmentation characteristics of MALDI Q/TOF MS/MS

A common feature associated with MALDI-MS analysis of the permethyl derivatives of *N*-acetyllactosamine (LacNAc)-based glycans is the in source prompt fragmentation which readily yields non-reducing terminal oxonium ions via directed cleavages at the GlcNAc. As with FAB-MS, this allows a facile mapping of the non-reducing terminal epitopes [4], and, importantly, they can be further selected for CID MS/MS sequencing. In general, however, these terminal LacNAc-based oxonium ions are of low *m/z* values (below *m/z* 800) and thus often masked by matrix peaks, except those that are further extended by a combination of sialylation, fucosylation, galactosylation, and/or additional LacNAc units. Among the most useful characteristics afforded by such pseudo MS^3 analysis is the elimination of C3-substituents from the GlcNAc and thus allowing a facile discrimination of type 1 (-Gal-3GlcNAc-) versus type 2 (-Gal-4GlcNAc) unit [4], as effectively demonstrated in past applications [37].

In contrast to in source fragment ions, molecular ions registered for the permethylated glycans are usually sodiated which in turn afford sodiated fragment ions when selected for MS/MS. As consistently demonstrated across all different kinds of MS instruments, the predominant fragment ions produced at low energy CID are always the B and Y ion pairs directed at HexNAc. The sodiated B ions are equivalent to the aforementioned oxonium ions which define the non-reducing terminal epitopes. These are complemented by the reducing terminal Y ions deriving from successive losses of non-reducing terminal epitopes (Fig. 1A and B, ion series marked with asteriks). Such multiple glycosidic cleavages is a characteristic feature of low energy CID-MS/MS of sodiated parent ions on the Q/TOF, which can be turned into advantages for distinguishing branching and multiple substitution by virtue of the *O*-Me tag introduced by permethylation in the first place. Typically for complex type N-glycans then, a sodiated trimannosyl core ion will be produced, the *m/z* value of which informs the number of free OH groups carried and thus the number of antenna originally attached (Fig. 1C). Another important cleavage site is the glycosidic bond between the two GlcNAcs of the chitobiose core. The resulting B ion may however be of low abundance and not detected since it is more commonly associated with additional losses of the non-reducing terminal epitopes which essentially gives rise to a second prominent series of reducing terminal ions devoid of the reducing end GlcNAc (Fig. 1A and B, ion series marked with #). If core fucosylation is present, a fucosylated Y_1 ion (*m/z* 474) will be additionally detected.

In short, the MALDI-MS/MS spectra of complex type N-glycans as acquired on a Q/TOF tend to be elegantly simple and most fragment ions can be readily assigned as either corresponding to B or Y ion or a combination of both, deriving from facile cleavages at HexNAc. However, several limitations are apparent, as a direct consequence of their dominance. Firstly, cleavage at sites other than HexNAc is often not detected which precludes full sequencing of stretches comprising several Hex and/or Fuc attached to delimiting HexNAc. Y ion corresponding to loss of the 3-arm Man can be detected at low abundance and appears to be more favorable than loss of the 6-arm Man, but not exclusively. Thus, in the representative MS/MS spectra shown in Fig. 1, signals at *m/z* 1402 and 2026 could be assigned as the Y ions derived through such cleavage for the tri- and tetra-antennary structures, respectively. This selectivity alone is however not sufficiently specific to allow discrimination of the antennary substituents on either 3- or 6-arm, especially since the implicated ion signals are often weak.

Similarly favored cleavages at the 3-arm relative to the 6-arm Man are also commonly observed as further loss of an Hex residue from the trimannosyl core ions. In the case of triantennary structure, as shown in Fig. 1A, such ions (*m/z* 939, 662) are useful indicator, of a 2,4-Man versus 2,6-Man types of triantennary branching. However, with either bi- or tetra-antennary structure, the respective cleavages at either arm will give isobaric products with the same number of free OH groups and thus non-discriminative. A related issue concerns the identification of bisecting GlcNAc. As shown in Fig. 1C, the trimannosyl core ions afforded cannot distinguish a bisected structure from a non-bisected one that is substituted with one additional antennae carrying a non-galactosylated terminal GlcNAc. The two alternative structural isomers contain the same number of free OH groups after losing all the antenna and the bisecting GlcNAc, if present.

Finally, while small O-glycans and other milk-derived oligosaccharides readily afford the sodiated C and Z ion pairs via glycosidic cleavages at Hex or Fuc 3-linked to HexNAc, the corresponding elimination of the C3-substituents from the antennary GlcNAc is less obvious to allow unambiguous assignment of a type 1 or Lewis A/B unit on N-glycans. Likewise, additional linkage informative cleavage ions such as those afforded by the cross ring cleavage ions are not normally observed with N-glycans. The low energy CID MS/MS analysis of permethylated N-glycans as afforded by MALDI Q/TOF is therefore most effective in mapping out the core structures and the complement of non-reducing terminal epitopes they carry but less conducive in deriving linkage specific cleavages for detailed sequencing. The dominance of B/Y ions is often at the expense of other types of cleavage ions. The problem is particularly acute as the molecular size increases for multiantennary N-glycans which eventually exceeds the affordable mass range of the quadrupole for parent ion isolation.

Fragmentation characteristics of MALDI TOF/TOF MS/MS

The first advantage of MALDI-TOF/TOF over Q/TOF for CID MS/MS is its ability to select parent ions of much higher *m/z* value. In practice, an extended range of *m/z* 4,000 to just below 10,000 is sufficient to cover most useful applications in glycan sequencing. An important consideration though is that, as the parent ion increases in size, the potential difference between the source acceleration voltage and the collision cell would also need to be elevated from the standard 1 or 2 kV settings in order to maintain the reported features of high energy CID MS/MS. Otherwise, the fragmentation achieved would essentially be of "low energy CID," very similar to that obtained on a Q/TOF with an important exception that multiple cleavages such as those due to successive losses of non-reducing terminal LacNAc-based units are not normally observed. This appears to be an important characteristic of TOF/TOF in that most cleavages including multiple bond ruptures are essentially derived from a single CID event, even at sufficiently high energy. The fragmentation mechanisms are thus commonly rationalized as being "concerted"

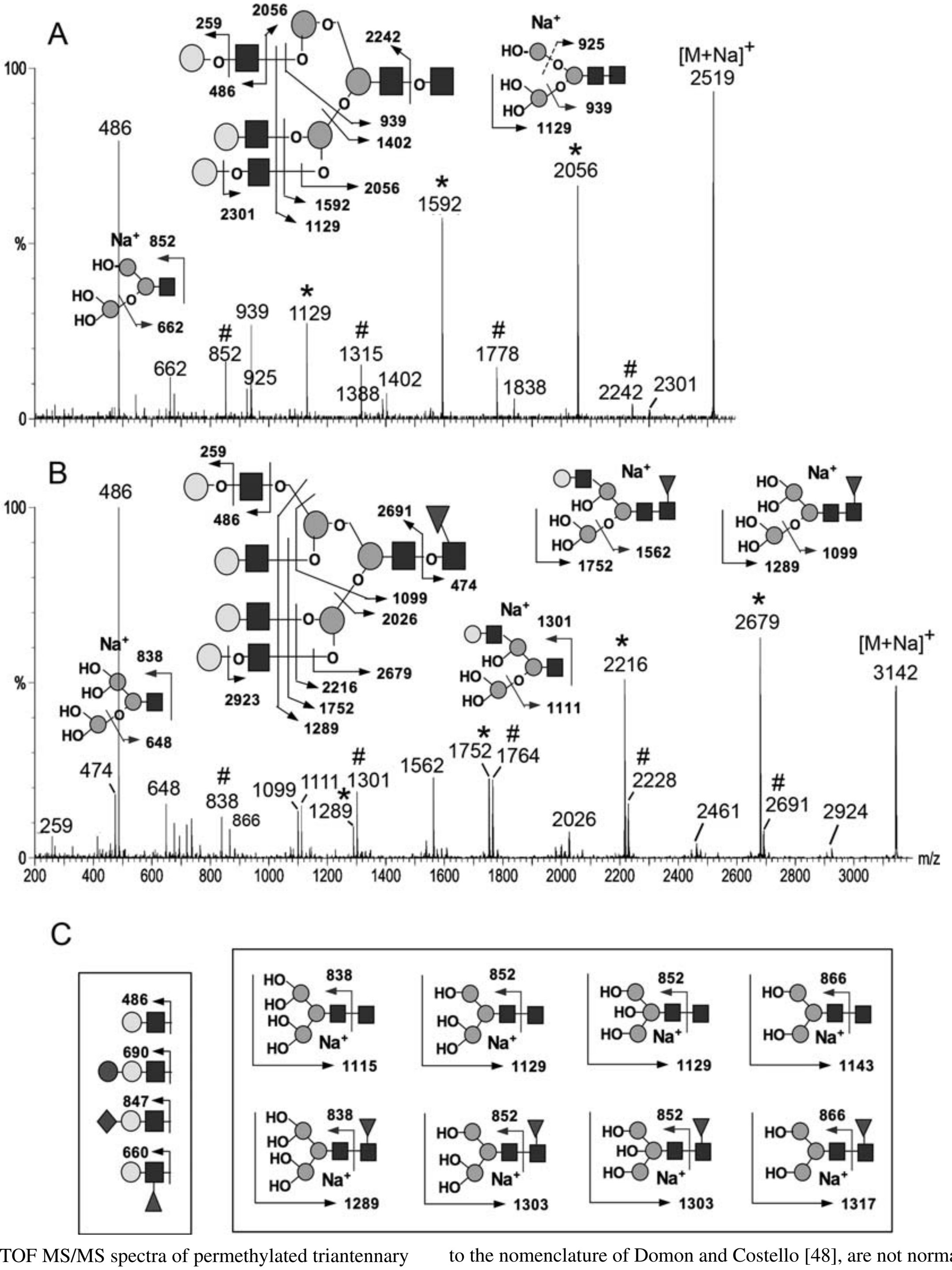

Fig. 1 MALDI Q/TOF MS/MS spectra of permethylated triantennary (A) and tetraantennary (B) complex type N-glycans. The predominant cleavages which generated the B and Y ions are schematically illustrated. The terminal LacNAc units are defined by the B ion, the *m/z* of which would reflect if it is further galactosylated, sialylated or fucosylated, as drawn on the left panel in (C). Y ion series resulting from consecutive losses of these non-reducing terminal LacNAc units from the parent ions are marked with (*) whereas those derived from the B ions at *m/z* 2242 and 2691 respectively for the tri- and tetra-antennary structures are marked with (#). The two representative examples demonstrate the respective final trimannosyl core ions that would be detected, depending on the number of antennae and whether the core is fucosylated, as further illustrated in (C). Other C, Z, X, and A ions, according to the nomenclature of Domon and Costello [48], are not normally detected. When the parent ions are of sufficient abundance, loss of terminal Hex from either the parent or primary fragment ions may be detected, *e.g. m/z* 2301, 1838 in (A) and *m/z* 2924, 2461 in (B). The extra core ion at *m/z* 866 in (B) indicated a probable additional presence of an isomeric biantennary structure although its definitive existence along the major tetraantennary structure could not be further substantiated by other corroborating ions such as the B ions for terminal $LacNAc_2$ and $LacNAc_3$ at *m/z* 935 and 1384, respectively, which were not detected at any significant level. Symbols used here and all other Figures are : circle ●, Hex; square ■, HexNAc; diamond ♦, NeuAc; triangle ▼, Fuc. Glycosidic oxygen atoms are drawn out only at cleavage sites to discriminate between cleavages at either side of the oxygen.

and confined to the same glycosyl residue, instead of independent CID events occurring at two distinct, unrelated sites.

With this in mind and taking the high energy CID MS/MS spectra of a representative selection of permethylated bi- and tri-antennary N-glycan standards (Figs. 2 and 3) as starting points, the various fragmentation characteristics reported in the literature [5,41,43–45] can be assimilated to formulate an easy-to-follow set of guidelines for *de novo* assignment of an otherwise seemingly complicated MS/MS spectrum. About the most significant changes in the fragmentation pattern when going from low energy to high energy CID is that the dominant B and Y ions are now accompanied by many other cleavage ions, including the ring cleavage ions and other "satellite" ions resulting from concerted elimination of substituents around the pyranose ring [43,45] (Fig. 2A). For ease of description and reference, the nomenclature introduced by Domon and Costello [49], for the A, B, C and X, Y, Z ions will be used in conjunction with the E, F, G ion nomenclature proposed by Spina *et al*. [43], for the so-called satellite ions. A related H ion is coined in this work since it is a natural extension from the E, F, G nomenclature for another of the satellite ion, while the loosely used term, D ion [50], is reserved here strictly for a particular kind of concerted double cleavage ions.

Reducing terminal ions

For the reducing terminal ions (Fig. 2A, **I**), the $^{1,5}X$ ions constitute the most reliable series of ions, invariably occurring at every glycosyl residue and thus afford a complete sequencing from the non-reducing terminus through to the trimannosyl core. The respective $^{1,5}X_3$ ions corresponding to cleavages at the 3-arm and 6-arm Man are usually quite abundant and easily identified while the $^{1,5}X_2$ ion deriving from cleavage at the branched β-Man occurs at either *m/z* 747 or 573, depending on whether the chitobiose core is fucosylated. Along the antennary sequence, the additional occurrence of Y ion is mostly restricted to HexNAc and thus often give rise to a pair of signals 28 u apart (the respective X and Y ions) which signifies a HexNAc site. At this HexNAc residue, the satellite ions resulting from eliminating in concert the attached glycosyl subsitutent along with another MeO- moiety are particularly abundant.

For a 4-linked HexNAc, the G and H ions differ by 14 u and thus can be easily identified as a characteristic pair of signals. A 3-linked GlcNAc would only give a G ion and not a H ion since both the 4- and 6-positions are not substituted. More importantly, when the GlcNAc is doubly or triply substituted, the G and H ion pairs will be shifted apart according to the mass of the substituents and thus be linkage informative. In the case of a terminal Lewis X on N-glycan (Fig. 3B), both the 4-linked Gal and 3-linked Fuc will be eliminated in concert to generate the G ion (*m/z* 2601), whereas only the 4-linked Gal will be eliminated along with the C6-OMe to give the H ion (*m/z* 2762). The latter ion is therefore shifted to 160 u higher instead of 14 u lower than the corresponding G ion. G, H and F ions can also occur at Hex residue but often less abundant. Notably, G and F ions which involve concerted elimination of 3,4- and 2,3-substituents respectively are indistinguishable for a 3-linked Hex but are useful to discriminate either of the two doubly substituted Hex residues. Thus the ion at *m/z* 3040 in Fig. 3A for an N-glycan carrying terminal Galα1-3Galβ1-4GlcNAc epitope can be equally assigned as G or F ion. As expected, the H ion is missing for this 3-linked Gal, as mentioned above, in contrast to the characteristic pair at 14 u apart (*m/z* 2836/2822) for the 4-linked GlcNAc.

In general then, the most abundant signals between the parent ion and the $^{1,5}X_3$ ion of the 3-arm or 6-arm Man can usually be confidently assigned according to the rules just described and, from which, a linkage specific sequence for the antenna can often be derived. Within this region, other minor signals can be further assigned but usually not without ambiguity and mostly provide no extra information for *de novo* sequencing of an unknown structure. In particular, the $^{1,5}X$ ions are often accompanied by many weaker signals at multiples of 14, 16, or 18 u below, some of which correspond to the Y, Z, F, G, H ions of adjacent Hex residues. Signals within this region will also become more complicated when an N-glycan under sequencing comprises isobaric structures or when its antenna are differently substituted. Essentially, the ambiguity then arises not from unpredictable cleavage but severe overlapping of isobaric ions. A different scenario occurs when the original parent ion signal is weak. Under such circumstances, only the Y ions at HexNAc and the $^{1,5}X$ ions may be detected and not the satellite ions (*e.g*. Fig. 3C).

Non-reducing terminal ions

The antennary sequence derived from the primary reducing terminal ions and their satellites should be corroborated by the non-reducing terminal ions (Fig. 2A, **II**). The sodiated B ions at HexNAc as afforded by low energy CID would normally remain as strong signals. Its identification is facilitated by a characteristic satellite signal at 71 u lower, attributable to the corresponding E ion which involves further elimination of the NMeAc substituent at C-2 of GlcNAc. Another commonly observed feature is the production of the oxonium ion in addition to or instead of the sodiated B ion, which is often accompanied by an ion corresponding to elimination of the 3-substituent or simply a MeOH moiety if not further substituted. Thus, the non-reducing terminal LacNAc unit gave rise to the B and E ions at *m/z* 486 and 415, respectively, as well as the oxonium ion at *m/z* 464, and 432 after elimination of a MeOH (Fig. 2B and C). The α3-galactosylated LacNAc unit afforded the B and E ion pairs at *m/z* 690 and 619 and the oxonium ion at *m/z* 668 (Fig. 3A) while the corresponding

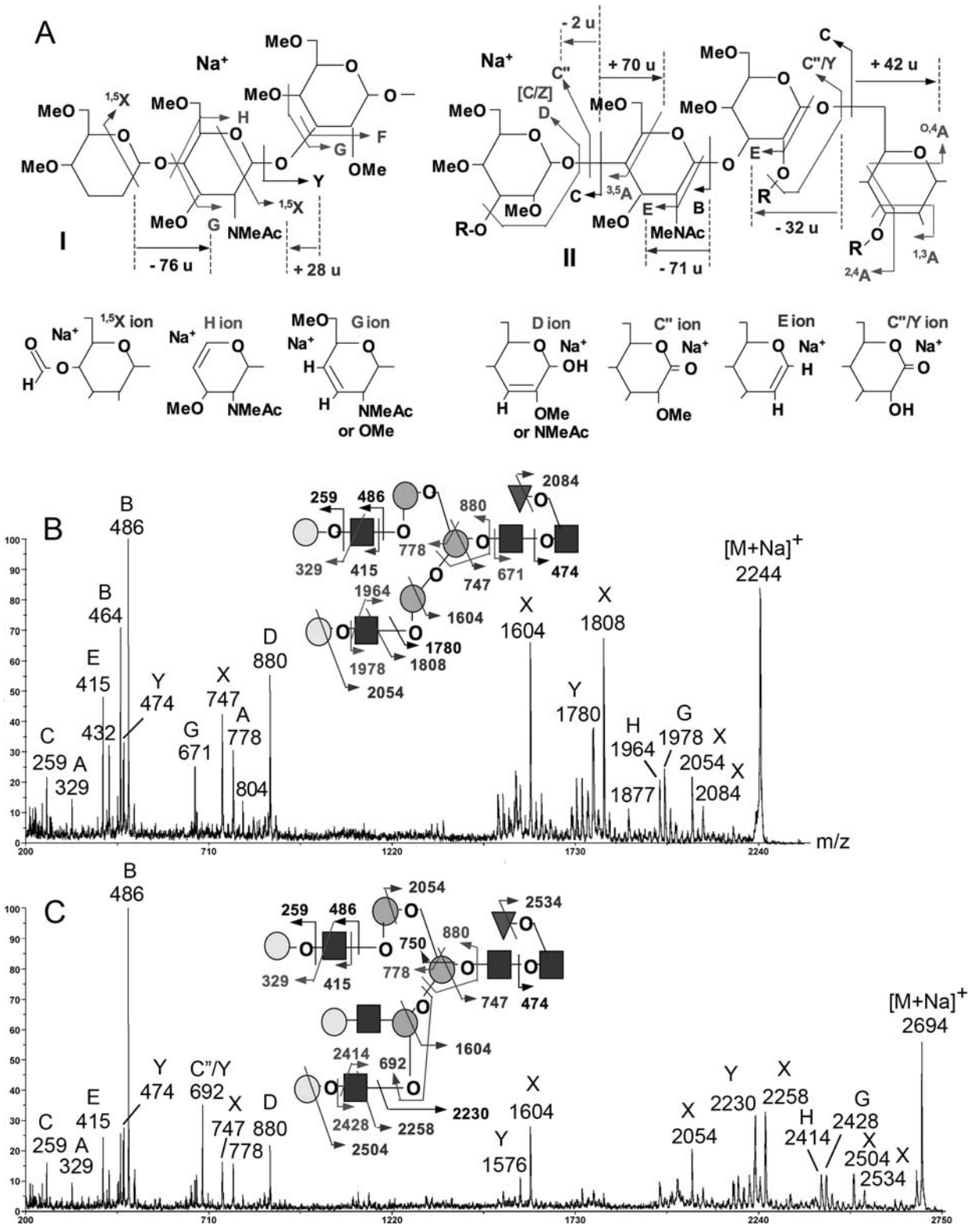

Fig. 2 Characteristic fragment ions afforded by MALDI TOF/TOF high energy CID MS/MS of permethylated complex type N-glycans. The reducing terminal (I) and non-reducing terminal (II) sets of fragment ions are schematically shown in (A), with nomenclature of the ions drawn from that proposed by Domon and Costello [49] and Spina *et al.* [43], as well as this work, for ease of description. Assignment of these fragment ions as afforded by the biantennary (B) and triantennary (C) complex type N-glycans is illustrated on the spectra by schematic drawing and the assigned peaks are labeled accordingly. The mass difference between ions constituting the characteristic pairs of signals is given in (A) so as to formulate an easy-to-follow pattern for signal assignment, as described in the text. Other types of X ions, *e.g.* the ^{O,2}X ion may occasionally be found but usually at very low abundance or absent.

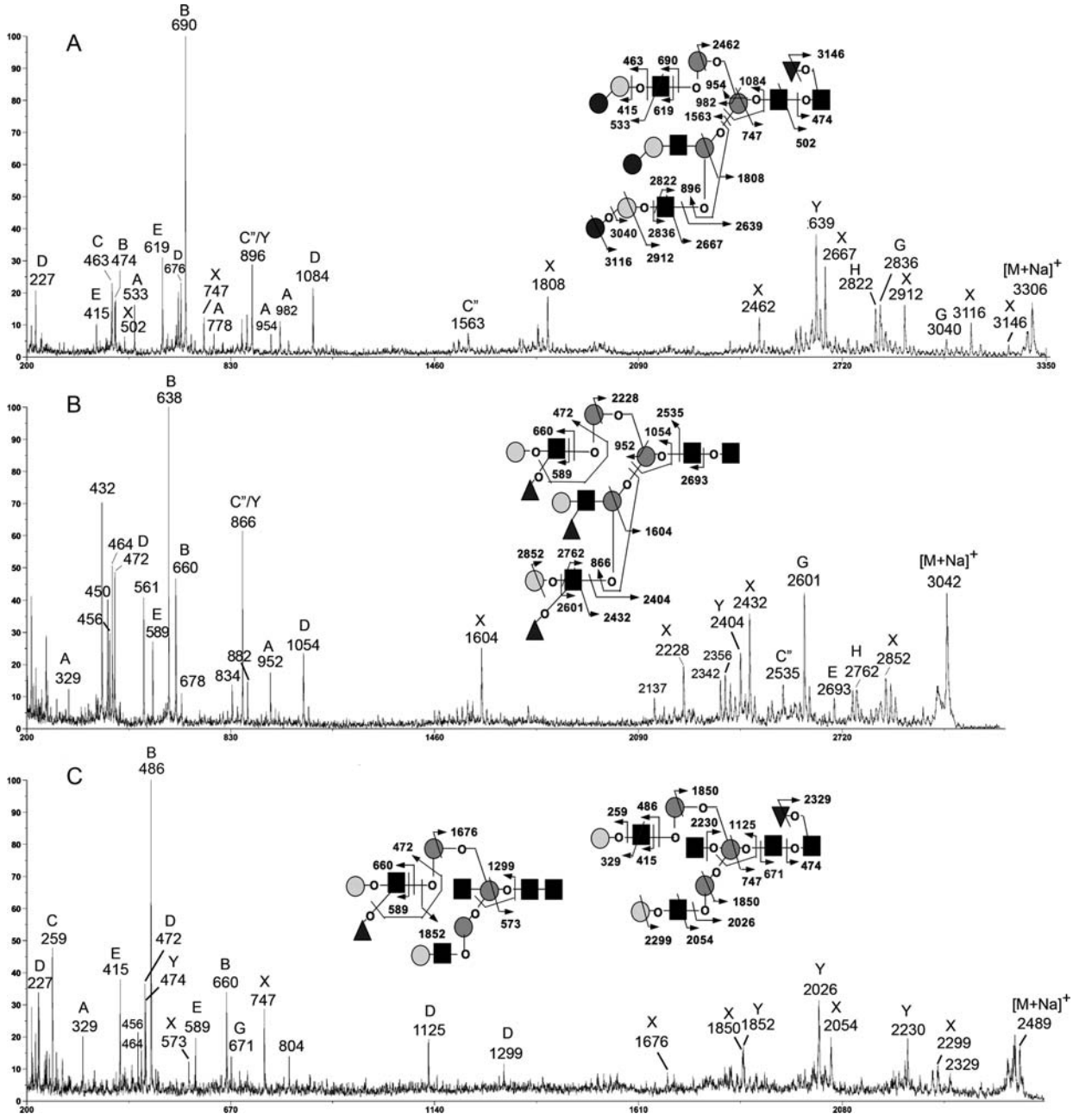

Fig. 3 MALDI TOF/TOF MS/MS spectra of permethylated complex type N-glycans carrying α3-Gal (A), Lewis X (B) and bisecting GlcNAc (C). The specific substituents in each example can be unambiguously assigned based on a combination of the characteristic fragment ions described. The triantennary structure carrying terminal Galα1-3Galβ1-4GlcNAc epitope (A) was obtained from rabbit erythrocytes; the triantennary structure with terminal Lewis X (B) was synthesized from a commercially available triantennary standard by incubation with α3-fucosyltransferase. The bisected biantennary structure in (C) was derived from the released N-glycan pool of a colonic adenocarcinoma cell line, Colo205; isomeric structures are clearly represented by the parent ion selected for MS/MS analysis.

ions for a terminal Lewis X unit occur at *m/z* 660, 589 and 638, respectively, further accompanied by elimination of the 3-linked Fuc from the oxonium ion to give the ion at *m/z* 432 (Fig. 3B). These sets of ions are not normally observed at sites other than HexNAc. Instead, at Hex residues, a weak C ion signal or one that contains two fewer H at 2 u lower [41,45] may be detected. The latter ion is hereafter referred to as C" ion and it is preferentially, but not exclusively, associated with glycosidic cleavage at a branched Hex residue *e.g.* the 3-arm Man of a triantennary structure or the 3,6-branched β-Man.

At lower abundance are the cross ring cleavage A ions which are very linkage informative except that they are often not reliably detected. On average, the most readily formed A ion is the ^{3,5}A ion which allows assignment of either a 4- or

6-linked linkage. The first ^{3,5}A ion at *m/z* 329 is indicative of a terminal Hex 4-linked to HexNAc, as in a terminal type 2 LacNAc or a Lewis X unit (Figs. 2B, C and 3B), although it could also be similarly formed for a Hex 6-linked to the next residue. A 6-linkage will be more confidently assigned if the ^{3,5}A ion is accompanied by an ^{O,4}A ion at 28 u lower, as often observed for the 6-arm Man (*m/z* 778 and 750 in Fig. 2B and C; *m/z* 982 and 954 in Fig. 3A). The absence of ^{3,5}A ion is consistent with but not an evidence for a 3-linked Hex, as in a terminal type 1 Gal-3GlcNAc unit. In the case of a terminal Galα1-3Galβ1-4GlcNAc unit, the $^{3,5}A_2$ ion at *m/z* 329 is missing whereas an $^{3,5}A_3$ ion can be detected at *m/z* 533 (Fig. 3A), as would be expected. It can be contented that a better support for a 3-linkage is the positive detection of the ^{2,4}A or ^{1,3}A ion (Fig. 2A) which, unfortunately, is usually not found. Nevertheless, a good quality high energy CID MS/MS spectrum of complex type N-glycan should carry with it sufficient information enshrined within the two complementary sets of reducing and non-reducing terminal ions to allow unambiguous sequence assignment of the antenna. Any branching can usually be easily detected and, in a majority of cases, complete with linkage information.

Internal or double cleavage ions

In contrast to the weak A ion signals, two other distinctive types of ions are usually detected as major signals which can respectively identify the 3- and 2-linked substituent. The first is named as the D ion which is used here to describe specifically the ion formed through a glycosidic cleavage in concert with elimination of the 3-substituent. Product wise, it can be viewed as an internal cleavage ion arising through a combination of B/Y or C/Z type of cleavages. An often cited case example is one that reported the D ion as specific ion related to double cleavages at the 3,6-branched β-Man, losing the chitobiose through glycosidic cleavage, coupled with elimination of the 3-arm [41,45]. Essentially, this generates the D ion which defines the 6-arm substituent. As shown in the two examples in Fig. 2B and C, both afforded the ion at *m/z* 880, accompanied by the ^{3,5}A ion at 102 u lower (*m/z* 778). Note that in the case of the triantennary standard, the corresponding D ion for an alternative isomer, namely one with 2,6-branched at the 3-arm was not detected. For the N-glycan which carries an additional Gal or Fuc on the antenna, the respective D ions are shifted to *m/z* 1084 and 1054, respectively (Fig. 3A and B), lending support to its assignment.

Importantly, we have since found that formation of D ion is not restricted to the 3,6-branched β-Man. It can actually be detected for each residue along the antenna but is more prominent, in terms of mass shift and abundance, when the cleavage site residue is substituted at the C3 position. Thus the N-glycan with Galα1-3Galβ1-4GlcNAc- termini afforded a rather strong signal at *m/z* 227 (Fig. 3A) which can be attributed to the internal β-Gal after losing both its glycosidic substituents at C1 and C3. The corresponding D ion for the GlcNAc was also detected at *m/z* 676, occurring at 14 u lower than the B ion. Importantly, in the case of a terminal Lewis X unit, the D ion for the GlcNAc occurs at *m/z* 472 which attests to a Fuc substituent at C3 position. Thus the formation of the D ion is reminiscent of the mechanism describing elimination of a 3-substituent from an oxonium ion of GlcNAc [4], with two important difference. First, it is not restricted to HexNAc as an oxonium ion often does. In fact, its first identification was founded on the specific cleavage ion of the β-Man of the trimannosyl core. Secondly, either one of the two oxygen atoms involved in the glycosidic cleavages is retained for the D ion which is best rationalized as a combination of C and Z–type cleavages although its mass is also compatible with a B and Y-type cleavages.

A real useful application for the D ion is to distinguish the bisecting GlcNAc, as shown in Fig. 3C which also typifies a recurring problem of isobaric mixtures when dealing with biological samples. The two complementary sets of reducing and non-reducing terminal ions as discussed above clearly identify at least two distinct isomers for this bisected biantennary structure, with the Fuc either located at one of the antenna as Lewis X, or on the core. The B and E ion pairs for LacNAc (*m/z* 486/415) and Lewis X (*m/z* 660/589) are both detected. So are the $^{1,5}X_2$ ions at *m/z* 747 and 573. Importantly, the D ions at *m/z* 1125 and 1299 indicate that a Fuc can either be present or absent on the 6-arm antenna, consistent with the structures drawn. To unambiguously localize the extra GlcNAc to the β-Man instead of an extra antenna with a non-galactosylated GlcNAc, an ^{O,4}A ion is ideally required which is absent here due to overall low abundance of the parent ion. In such case, however, the absence of $^{1,5}X_3$ ion (cleavage at either the 3- or 6-arm Man) which carries an additional HexNAc would still provide strong evidence that the antennae are only extended by either a LacNAc ($^{1,5}X_3$ ion at *m/z* 1850) or Lewis X ($^{1,5}X_3$ ion at *m/z* 1676).

A second "double" cleavage ion which has also been reported previously [41], can be rationalized as arising from glycosidic cleavage in concert with losing the 2-linked substituent. The product ion, referred to as C"/Y ion here, is very similar to the E ion with a few notable differences. First, both oxygen atoms at the cleavage sites are retained and not eliminated as in E ion, and therefore occurring at 32 u higher than the E ion. The minus 32 u satellite signal is usually of lower abundance but indicates that E ions can also be formed at a Hex residue that is 2-linked. Second, it is not formed at GlcNAc which carries an NMeAc at C2, and which favors instead an E ion. Since there are not many naturally occurring Hex residue that is 2-substituted apart from the Man of the trimannosyl core, this ion is mostly observed only with tri- and tetraantennary structures. In these cases, the antenna

is 2-linked to Man will be lost, and thus the C"/Y ion essentially define the substituents on the antenna 4-linked to 2,4-Man, or the antenna 6-linked to 2,6-Man. It is most useful for triantennary structure since it allows an elegant way to discriminate the additional third antennary structure that is not 2-linked to Man. As shown here in the three representative case examples, the C"/Y ion for the triantennary structures carrying terminal LacNAc, α3-galactosylayed LacNAc and Lewis X units occur at *m/z* 692, 896 and 866, respectively (Figs. 2B, C and 3A, B). For tetraantennary structures, the same rule holds but the ion itself does not allow discrimination between a structure 4-linked or 6-linked to the Man, unless assigned in conjunction with other fragment ions.

Sialylated N-glycans

An advantage with analyzing permethyl derivatives is that sialylated glycans will essentially behave just like neutral glycans without imposing the negative charge which often leads to its poor ionization and/or facile loss in positive ion mode. In applying the high energy CID MS/MS to a variety of sialylated N-glycans (Fig. 4), we have found that all the fragmentation characteristics established and described above hold true. It should however be noted that the ^{1,5}X ion resulting from ring cleavage at the sialic acid now incorporates an additional –COOMe moiety which therefore occurs at 86 u, and not 28 u, higher than the corresponding Y ion. This signal pair of 86 u apart, produced via loss of a terminal sialic acid residue, can be easily identified as the first major signals going down in mass from the parent ion. A G ion will next be detected if the sialic acid is 3-linked to the penultimate Gal but not if it is 6-linked. This is followed by the characteristic pair of G and H ions of 14 u apart resulting from cleavages around the GlcNAc, the X and Y ion pairs of 28 u apart due to loss of the NeuAc2-3/6Gal-GlcNAc- moiety, and finally the $^{1,5}X_3$ ion from cleavages at the 3- and 6-arm Man. Importantly, when heterogeneity exists due to disialylation on one of the antennae, two distinct sets of X and Y ion pairs related to loss of the respective mono- and disialylated antennae are clearly detectable (Fig. 4B and C). This unambiguously locates the extra sialic acid substituent on the internal GlcNAc.

As before, further corroborative sequencing data for the antenna can be obtained from the non- reducing terminal ions. Each of the sialylated structures would afford an abundant ion corresponding to the terminal NeuAc or NeuGc. Interestingly, the oxonium type ions at *m/z* 376 and 406, for $NeuAc^+$ and $NeuGc^+$ respectively, seems to be more readily formed than the sodiated B_1 ions at *m/z* 398 and 428, although both are detected. The oxonium ions are invariably accompanied by elimination of a MeOH moiety to give the strong signals at *m/z* 344 and 374. Another characteristic ion that are consistently detected comprise one at *m/z* 356 and 386 for NeuAc and NeuGc carrying glycans respectively. These ions can be tentatively rationalized as the sodiated C_1 ion for the terminal NeuAc/NeuGc, but with concerted elimination of the –COOMe moiety [5]. The sodiated B and E ions for the NeuAc/NeuGc-Gal-GlcNAc epitope can be detected at *m/z* 847/877 and 776/806 respectively while the corresponding oxonium ion at *m/z* 825/855 are also readily formed. For structures also carrying a disialylated antenna, a third B and E ion set is present at *m/z* 1208 and 1137 for one disialylated with two NeuAc (Fig. 4B) and *m/z* 1268 and 1197 for one disialylated with two NeuGc (Fig. 4C). The C_2 and/or C" ions at 2 u less for glycosidic cleavage at the Gal is also well represented by the ions at *m/z* 620 or 650 for the NeuAc/NeuGc variants.

Of particular interest, the ions at *m/z* 629 (Fig. 4B) and 659 (Fig. 4C) can be assigned as corresponding to the D ions formed at the NeuAc and NeuGc-sialylated internal GlcNAc, respectively, which is consistent with the well established sequence of Neu2-3Gal1-3(Neu2-6)GlcNAc [51]. Concerted elimination of the C3-substituent from GlcNAc would facilitate the formation of the D ion which is characteristic of the implicated disialylated antenna. In N-glycans derived from the serum of mice harboring an implanted tumor, this disialylation was found to increase relative to those derived from normal mice. Our MS/MS analysis (Fig. 4C) now provides a rapid, sensitive and definitive method to unambiguously detect such epitope. The corresponding D ion that would have been formed if the sialylated GlcNAc is not 3-linked but 4-linked as in type 2 LacNAc unit could not be detected. On the other hand, the D ions at *m/z* 833/863 are indicative of a NeuAc/NeuGc-Gal-4GlcNAc sequence for the monosialylated antenna.

For the tetrasialylated triantennary N-glycans derived from bovine fetuin, it is well established that the single disialylated antenna is attached to C4 of the 3-arm Man [51,52]. A C"/Y ion was indeed afforded at *m/z* 1414, accompanied by E ion at *m/z* 1382, lending credential to its assignment (Fig. 4B). For the corresponding trisialylated triantennary structure, these two ions are shifted to *m/z* 1053 and 1021, respectively (Fig. 4A). The absence of this C"/Y and E ion pair for the monosialylated antennary sequence in Fig. 4B is in full agreement with the exclusive presence of the disialylated antenna on the C4 of the 3-arm Man. Accordingly, the D ion at the 3,6-branched β-Man (*m/z* 1241), accompanied by the ^{3,5}A ion at *m/z* 1139, provides further evidence for the exclusive presence of a monosialylated antenna the 6-arm. A disialylated antenna a non-branched 3- or 6-arm Man would also give rise to $^{1,5}X_3$ ion that was not detected. Instead, the two $^{1,5}X_3$ ions at *m/z* 2963 and 1791 indicate that one arm is extended by a monosialylated antenna while the other is extended by 2 antennae with 3 NeuAc residues. Thus, the combination of ^{1,5}X, D and C"/Y ions affords a definitive localization of the variably sialylated antennae which is

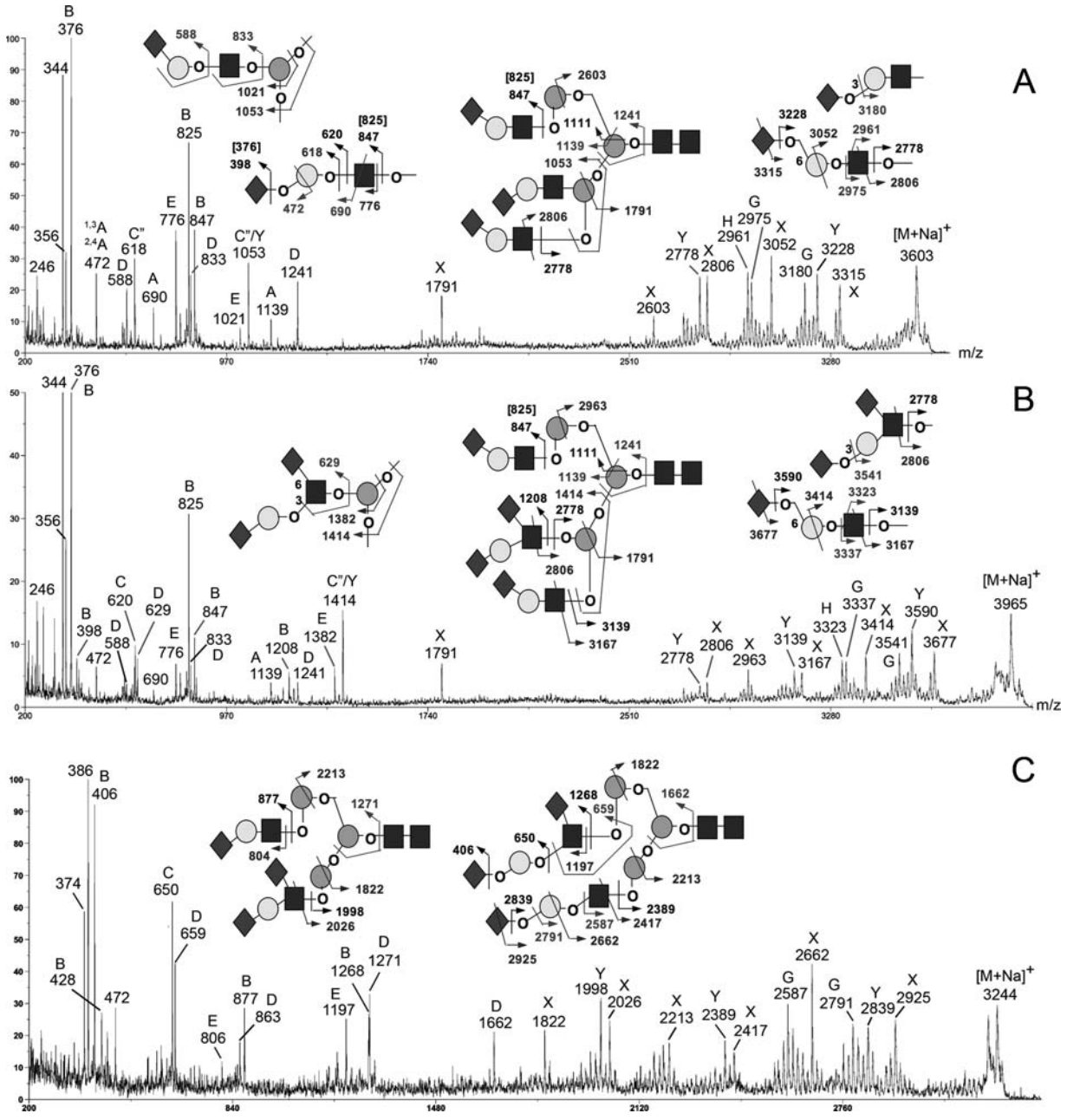

Fig. 4 MALDI TOF/TOF MS/MS spectra of permethylated sialylated complex type N-glycans. The trisialylated triantennary (A) and tetrasialylated triantennary (B) N-glycans are from bovine fetuin. MS/MS were directly performed on molecular ions detected by MALDI-MS analysis of the released N-glycans without further fractionation of the various isomers known to exist and differ primarily in their α2-3 versus α2–6 sialylation. Thus both terminal sialylation are present on the parent ion analyzed. The disialylated antenna however exclusively of the sequence NeuAcα2-3Galβ1-3(NeuAcα2–6)GlcNAc, whereas the monosialylated antennae are mostly based on type 2 LacNAc unit [51,52]. The parent ion corresponding to a trisialylated biantennary N-glycan (C) was selected from total serum N-glycan pool of mice harboring a breast tumor, which has been mapped to show an increased in sialylation relative to those from normal mice. Also increased in relative amounts are tetrasialylated biantennary structures with disialylated antenna on both arms (data not shown)

applicable to all other complex type structures with different antennary substituents. In the case of the trisialylated biantennary structures from mouse serum (Fig. 4C), the presence of both D ions at *m/z* 1271 and 1662 indicate that the disialylated antennae can be equally distributed on either arm.

As a final application example, the established high energy CID MS/MS fragmentation pattern was used to sequence the rather unusual complex type N-glycans from zebrafish embryos. Previous MS studies have revealed that the major complex type N-glycans are biantennary, with both antennae

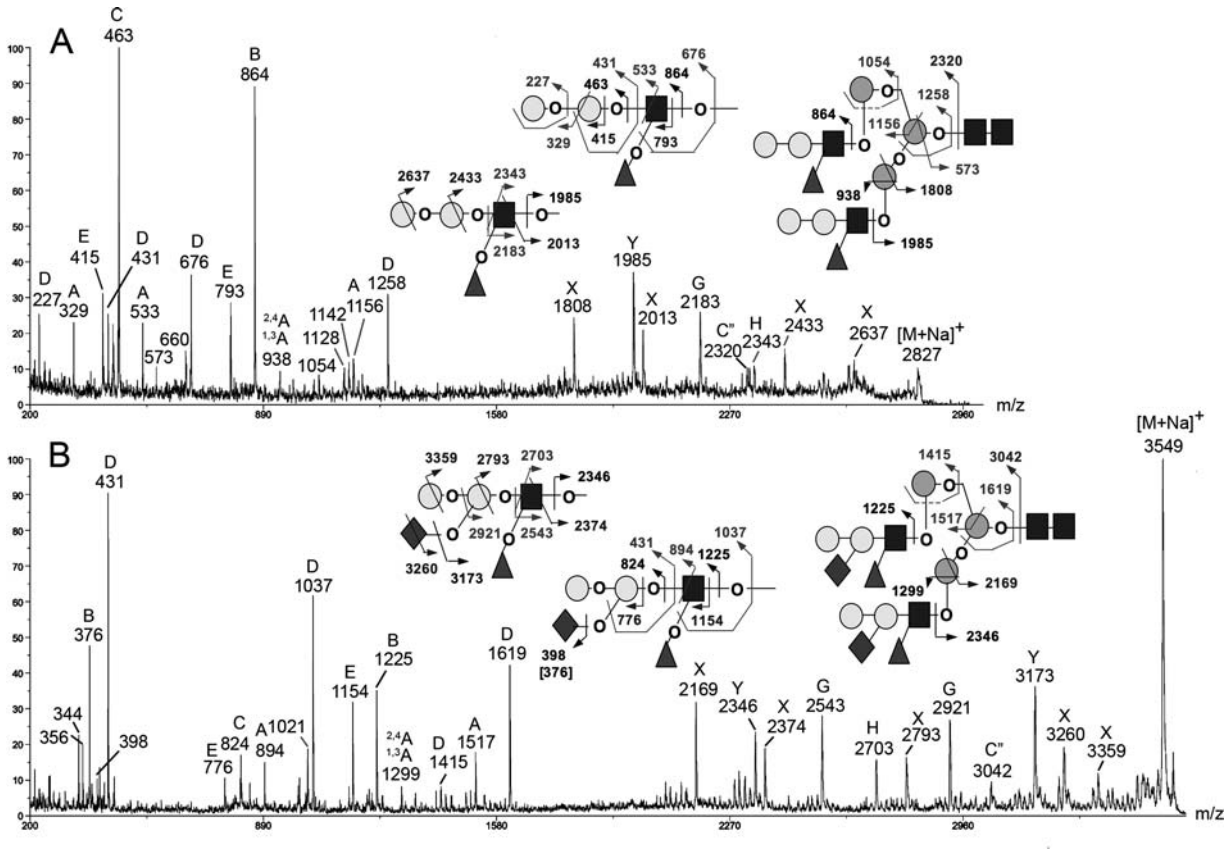

Fig. 5 MALDI TOF/TOF MS/MS spectra of permethylated complex type N-glycans with sialylated, fucosylated and galactosylated terminal LacNAc unit after (A) and before (B) enzymatic desialylation. The structures of the unusual N-glycans from zebrafish embryos have previously been characterized and deduced to be as drawn here. Both NeuGc and NeuAc sialylated structures were detected by MALDI MS profiling but only MS/MS on the NeuAc-sialylated structure is shown (B). Desialylation was effected by treating the N-glycan pool with neuraminidase. Note that the D ions as drawn can be formed practically at each site but most conspicuous when associated with 3-substituted residues. The cluster of signals at *m/z* 344, 356, 376 and 398 in (B) are derived from terminal NeuAc, as described in Fig. 4.

extended by a $NeuAc_1Fuc_1Hex_2HexNAc_1$ moiety. Subsequent MS/MS studies on a MALDI Q/TOF before and after desialylation, coupled with β-galactosidase digestion and/or chemical defucosylation led to identification of a Galβ1-4Galβ1-4(Fucα1-3)GlcNAc epitope but the localization of the sialic acid to the internal Gal residue can only be determined after linkage analysis revealing the presence of a 3,4- disubstituted Gal [46]. Essentially, the low energy CID MS/MS analysis could not distinguish between sialylation on either of the two Gal since a critical glycosidic cleavage between the two Gal could not occur.

Seeking corroborative evidence for the assigned structure, unambiguous sequencing can now be rapidly achieved by high energy CID MS/MS, relying on the array of ions described above. As shown in Fig. 5A for the desialylated biantennary N-glycan, two ^{1,5}X ions at *m/z* 2637 and 2433 were detected respectively for the two consecutive Gal residues. The next ^{1,5}X ion at *m/z* 2013, which pairs with the Y ion at *m/z* 1985 at 28 u lower, clearly define a fucosylated HexNAc unit sandwiched between the terminal Gal-Gal and the 3/6-arm Man. Around the HexNAc residue, a prominent G ion is detected at *m/z* 2183, fully consistent with elimination of both 3- and 4- substituents. The absence of an H ion at 14 u lower, but shifted instead to *m/z* 2343 is further evidence for a Fuc 3-linked to GlcNAc and thus retained in the formation of the H ion but not G ion. The 3,4-substituted GlcNAc is also apparent from the detection of an abundant D ion at *m/z* 676 which corresponds to a Hex_2-HexNAc-OH moiety, having eliminated the Fuc substituent from C3 of the HexNAc. Other supportive non-reducing terminal ions as schematically illustrated on Fig. 5A include the abundant C_2 ion at *m/z* 463 (Hex_2-OH), the D ion at *m/z* 431 (Hex_2-OH with further elimination of a MeOH moiety), the B and E ion pair at *m/z* 864/793 ($Hex_2Fuc_1HexNAc$), the ^{3,5}A ions at *m/z* 329 and 533 supportive of the respective 4-linkage, and the ^{1,3}A ion at *m/z* 938, consistent with the 2-linkage.

Notably, the D ion at *m/z* 431 is retained as a very prominent signal in the spectrum of the sialylated sample (Fig. 5B), providing a strong evidence for the sialic acid being attached to the C3-position of the internal Gal and thus eliminated during the formation of D ion. In accordance with this assignment, the next D ion of the GlcNAc occurs at *m/z* 1037 which

is exactly a NeuAc increment from the corresponding D ion (*m/z* 676) afforded by the desialylated sample. Likewise, the C_2 ion is detected at *m/z* 824, followed by the ^{3,5}A ion at *m/z* 894, both shifted a NeuAc increment. This ensemble of non-reducing terminal ions collectively enable an unequivocal sequence and linkage assignment of the terminal epitope and further corroborated by the reducing terminal ions comprising the ^{1,5}X, Y, G and H ions. The detection of ^{1,5}X ion for cleavage at terminal Hex indicates that the NeuAc is not capping the terminal Gal. The strong G ion signal at *m/z* 2921 is consistent with the internal Hex being 3,4- disubstituted. Likewise for the G ion of the GlcNAc at *m/z* 2543 with its corresponding H ion shifted to *m/z* 2703. Finally, the D ions corresponding to cleavage at the 3,6-branched β-Man are very prominent for both sialylated and desialylated samples, both complemented further by detection of the ^{3,5}A ion.

Conclusion

More than a decade since the first serious attempts on high energy CID MS/MS based on FAB-ionization on 4 sector tandem mass spectrometers, the many promises then glimpsed and can now be practically realized at a sensitivity level that is within the realm of biological applications. A MALDI high energy CID-MS/MS implemented on a TOF/TOF instrument should now be viewed as one of the two most effective platforms for *de novo* sequencing, along with the multistage MS^n performed on an ion trap device. Single stage low energy CID-MS/MS on an instrument such as Q/TOF nevertheless still retains its attractiveness as the fragmentation pattern afforded is relatively simple. The resulting spectrum is thus easy to interpret and an overall picture for the unknown structure under investigation can be readily derived. The multiple cleavages producing the characteristic core ions are as important and diagnostic as the terminal B and Y ions in mapping the non-reducing terminal substituents. This is often underappreciated and constitutes a distinctive advantage afforded by analyzing permethyl derivatives.

In retrospect, most of the additional cleavages afforded at high energy CID have been noted previously in much earlier work although not all ions are produced equally abundant. The expected B, D, ^{1,5}X, and Y ions are always very prominent and, provided the parent ion is not too weak to begin with, the satellite G, H and E ions are also readily detected to afford a highly predictable MS/MS spectrum for facile *de novo* sequencing, as demonstrated here. For the tri- and tetraantennary structures, the C"/Y ions are also reliably formed to allow easy discrimination of the antenna 2-linked and not 2-linked to the Man. On the other hand, we tend to find that the A ions other than ^{3,5}A ions are less readily formed and their low abundance often preclude their usefulness. Several other minor signals will always be present that may not be readily assigned with confidence, but these are deemed not compromising the otherwise very informative rich MS/MS spectra.

In short, we have identified those fragment ions that are most consistently produced and most sequence-informative for complex type N-glycans, including those of sialylated ones. We demonstrated their practical usage in sequencing novel structures, as well as to discriminate isobaric structures and to identify the existence of particular structural determinants, as often entailed by glycomic analysis. The relative ease and sensitivity that we can now rapidly sequence and define the respective linkages of the terminal unit by MS/MS as shown here for the galactosylated sialyl Lewis X epitope in zebrafish N-glycans, is a reflection of how much we have progressed since this structural unit was first identified on the fertilized eggs of Medaka fish [53], more than a decade ago by Prof. Yasuo Inoue's group, in collaboration with Anne Dell's team.

Acknowledgments This work is supported by an Academia Sinica GRC (Genomic Research Center) Program Project Grant to KHK who holds a joint appointment at GRC. Mass spectrometry analyses were performed at the Core Facilities for Proteomics Research located at the Institute of Biological Chemistry, Academia Sinica, supported by a Taiwan National Science Council grant (NSC 93-3112-B-001-010-Y; NSC94-3112-B001-009-Y) and the Academia Sinica. Preparation and provision of biological samples by collaborators as listed in the Materials section is gratefully acknowledged.

References

1. Sutton-Smith, M., Morris, H.R., Grewal, P.K., Hewitt, J.E., Bittner, R.E., Goldin, E., Schiffmann, R., Dell, A.: MS screening strategies: Investigating the glycomes of knockout and myodystrophic mice and leukodystrophic human brains. Biochem. Soc. Symp. **69**, 105–15 (2002)
2. Kochetkov, N.K., Chizhov, O.S.: Mass spectrometry of carbohydrate derivatives. Adv. Carbohydr. Chem. Biochem. **21**, 39–93 (1966)
3. Egge, H., Peter-Katalinic, J.: Fast atom bombardment mass spectrometry for structural elucidation of glycoconjugates. Mass Spectrom. Rev. **6**, 331–93 (1987)
4. Dell, A.: F.A.B.-mass spectrometry of carbohydrates. Adv. Carbohydr. Chem. Biochem. **45**, 19–72 (1987)
5. Lemoine, J., Fournet, B., Despeyroux, D., Jennings, K.R., Rosenberg, R., de Hoffmann, E.: Collision-induced dissociation of alkali metal cationized and permethylated oligosaccharides: Influence of the collision energy and of the collision gas for the assignment of linkage position. J. Am. Soc. Mass Spectrom. **4**(3), 197–302 (1993)
6. Reinhold, V.N., Reinhold, B.B., Chan, S.: Carbohydrate sequence analysis by electrospray ionization-mass spectrometry. Methods Enzymol. **271**, 377–402 (1996)
7. Weiskopf, A.S., Vouros, P., Harvey, D.J.: Characterization of oligosaccharide composition and structure by quadrupole ion trap mass spectrometry. Rapid Commun. Mass Spectrom. **11**(14), 1493–504 (1997)
8. Viseux, N., de Hoffmann, E., Domon, B.: Structural analysis of permethylated oligosaccharides by electrospray tandem mass spectrometry. Anal. Chem. **69**(16), 3193–98 (1997)

9. Weiskopf, A.S., Vouros, P., Harvey, D.J.: Electrospray ionization-ion trap mass spectrometry for structural analysis of complex N-linked glycoprotein oligosaccharides. Anal. Chem. **70**(20), 4441–47 (1998)
10. Viseux, N., de Hoffmann, E., Domon, B.: Structural assignment of permethylated oligosaccharide subunits using sequential tandem mass spectrometry. Anal. Chem. **70**(23), 4951–59 (1998)
11. Morelle, W., Faid, V., Michalski, J.C.: Structural analysis of permethylated oligosaccharides using electrospray ionization quadrupole time-of-flight tandem mass spectrometry and deutero-reduction. Rapid Commun. Mass Spectrom. **18**(20), 2451 (2004)
12. Ashline, D., Singh, S., Hanneman, A., Reinhold, V.: Congruent Strategies for Carbohydrate Sequencing. 1. Mining Structural Details by MS(n). Anal. Chem. **77**(19), 6250–62 (2005)
13. Harvey, D.J.: Collision-induced fragmentation of underivatized N-linked carbohydrates ionized by electrospray. J. Mass Spectrom. **35**(10), 1178–90 (2000)
14. Chai, W., Piskarev, V., Lawson, A.M.: Negative-ion electrospray mass spectrometry of neutral underivatized oligosaccharides. Anal. Chem. **73**(3), 651–57 (2001)
15. Sagi, D., Peter-Katalinic, J., Conradt, H.S., Nimtz, M.: Sequencing of tri- and tetraantennary N-glycans containing sialic acid by negative mode ESI QTOF tandem MS. J. Am. Soc. Mass Spectrom. **13**(9), 1138–48 (2002)
16. Chai, W., Piskarev, V., Lawson, A.M.: Branching pattern and sequence analysis of underivatized oligosaccharides by combined MS/MS of singly and doubly charged molecular ions in negative-ion electrospray mass spectrometry. J. Am. Soc. Mass Spectrom. **13**(6), 670–79 (2002)
17. Robbe, C., Capon, C., Coddeville, B., Michalski, J.C.: Diagnostic ions for the rapid analysis by nano-electrospray ionization quadrupole time-of-flight mass spectrometry of O-glycans from human mucins. Rapid Commun. Mass Spectrom. **18**(4), 412–20 (2004)
18. Harvey, D.J.: Fragmentation of negative ions from carbohydrates: part 1. Use of nitrate and other anionic adducts for the production of negative ion electrospray spectra from N-linked carbohydrates. J. Am. Soc. Mass Spectrom. **16**(5), 622–30 (2005)
19. Harvey, D.J.: Fragmentation of negative ions from carbohydrates: part 2. Fragmentation of high-mannose N-linked glycans. J. Am. Soc. Mass Spectrom. **16**(5), 631–46 (2005)
20. Harvey, D.J.: Fragmentation of negative ions from carbohydrates: Part 3. Fragmentation of hybrid and complex N-linked glycans. J. Am. Soc. Mass Spectrom. **16**(5), 647–59 (2005)
21. Harvey, D.J.: N-(2-diethylamino)ethyl-4-aminobenzamide derivative for high sensitivity mass spectrometric detection and structure determination of N-linked carbohydrates. Rapid Commun. Mass Spectrom. **14**(10), 862–71 (2000)
22. Harvey, D.J.: Electrospray mass spectrometry and fragmentation of N-linked carbohydrates derivatized at the reducing terminus. J. Am. Soc. Mass Spectrom. **11**(10), 900–15 (2000)
23. Lattova, E., Perreault, H.: Profiling of N-linked oligosaccharides using phenylhydrazine derivatization and mass spectrometry. J. Chromatogr. A **1016**(1), 71–87 (2003)
24. Takegawa, Y., Ito, S., Yoshioka, S., Deguchi, K., Nakagawa, H., Monde, K., Nishimura, S.I.: Structural assignment of isomeric 2-aminopyridine-derivatized oligosaccharides using MSn spectral matching. Rapid Commun. Mass Spectrom. **18**(4), 385–91 (2004)
25. Morelle, W., Michalski, J.C.: Sequencing of oligosaccharides derivatized with benzylamine using electrospray ionization-quadrupole time of flight-tandem mass spectrometry. Electrophoresis **25**(14), 2144–55 (2004)
26. Morelle, W., Page, A., Michalski, J.C.: Electrospray ionization ion trap mass spectrometry for structural characterization of oligosaccharides derivatized with 2-aminobenzamide. Rapid Commun. Mass Spectrom. **19**(9), 1145–58 (2005)
27. Harvey, D.J.: Collision-induced fragmentation of negative ions from N-linked glycans derivatized with 2-aminobenzoic acid. J. Mass Spectrom. **40**(5), 642–53 (2005)
28. Kameyama, A., Kikuchi, N., Nakaya, S., Ito, H., Sato, T., Shikanai, T., Takahashi, Y., Takahashi, K., Narimatsu, H.: A Strategy for identification of oligosaccharide structures using observational multistage mass spectral library. Anal. Chem. **77**(15), 4719–25 (2005)
29. Dell, A., Morris, H.R.: Glycoprotein structure determination by mass spectrometry. Science **291**(5512), 2351–56 (2001)
30. Harvey, D.J., Bateman, R.H., Bordoli, R.S., Tyldesley, R.: Ionisation and fragmentation of complex glycans with a quadrupole time-of-flight mass spectrometer fitted with a matrix-assisted laser desorption/ionisation ion source. Rapid Commun. Mass Spectrom. **14**(22), 2135–42 (2000)
31. Loboda, A.V., Krutchinsky, A.N., Bromirski, M., Ens, W., Standing, K.G.: A tandem quadrupole/time-of-flight mass spectrometer with a matrix-assisted laser desorption/ionization source: Design and performance. Rapid Commun. Mass Spectrom. **14**(12), 1047–57 (2000)
32. Medzihradszky, K.F., Campbell, J.M., Baldwin, M.A., Falick, A.M., Juhasz, P., Vestal, M.L., Burlingame, A.L.: The characteristics of peptide collision-induced dissociation using a high-performance MALDI-TOF/TOF tandem mass spectrometer. Anal. Chem. **72**(3), 552–58 (2000)
33. Harvey, D.J., Postsource decay fragmentation of N-linked carbohydrates from ovalbumin and related glycoproteins. J. Am. Soc. Mass Spectrom. **11**(6), 572–77 (2000)
34. Naven, T.J., Harvey, D.J., Brown, J., Critchley, G.: Fragmentation of complex carbohydrates following ionization by matrix-assisted laser desorption with an instrument fitted with time-lag focusing. Rapid Commun. Mass Spectrom. **11**(15), 1681–86 (1997)
35. Hanrahan, S., Charlwood, J., Tyldesley, R., Langridge, J., Bordoli, R., Bateman, R., Camilleri, P.: Facile sequencing of oligosaccharides by matrix-assisted laser desorption/ionisation on a hybrid quadrupole orthogonal acceleration time-of-flight mass spectrometer. Rapid Commun. Mass Spectrom. **15**(14), 1141–51 (2001)
36. Suzuki, N., Khoo, K.H., Chen, C.M., Chen, H.C., Lee, Y.C.: N-glycan structures of pigeon IgG: A major serum glycoprotein containing Galalpha1–4 Gal termini. J. Biol. Chem. **278**(47), 46293–306 (2003)
37. Terada, M., Khoo, K.H., Inoue, R., Chen, C.I., Yamada, K., Sakaguchi, H., Kadowaki, N., Ma, B.Y., Oka, S., Kawasaki, T., Kawasaki, N.: Characterization of oligosaccharide ligands expressed on SW1116 cells recognized by mannan-binding protein. A highly fucosylated polylactosamine type N-glycan. J. Biol. Chem. **280**(12), 10897–913 (2005)
38. Kui Wong, N., Easton, R.L., Panico, M., Sutton-Smith, M., Morrison, J.C., Lattanzio, F.A., Morris, H.R., Clark, G.F., Dell, A., Patankar, M.S.: Characterization of the oligosaccharides associated with the human ovarian tumor marker CA125. J. Biol. Chem. **278**(31), 28619–634 (2003)
39. Zhang, H., Singh, S., Reinhold, V.N.: Congruent strategies for carbohydrate sequencing. 2. FragLib: An MS(n) spectral library. Anal. Chem. **77**(19), 6263–70 (2005)
40. Lapadula, A.J., Hatcher, P.J., Hanneman, A.J., Ashline, D.J., Zhang, H., Reinhold, V.N.: Congruent strategies for carbohydrate sequencing. 3. OSCAR: An algorithm for assigning oligosaccharide topology from MS(n) data. Anal. Chem. **77**(19), 6271–79 (2005)
41. Harvey, D.J., Bateman, R.H., Green, M.R.: High-energy collision-induced fragmentation of complex oligosaccharides ionized by matrix-assisted laser desorption/ionization mass spectrometry. J. Mass Spectrom. **32**(2), 167–87 (1997)

42. Mechref, Y., Novotny, M.V., Krishnan, C.: Structural characterization of oligosaccharides using MALDI-TOF/TOF tandem mass spectrometry. Anal. Chem. **75**(18), 4895–903 (2003)
43. Spina, E., Sturiale, L., Romeo, D., Impallomeni, G., Garozzo, D., Waidelich, D., Glueckmann, M.: New fragmentation mechanisms in matrix-assisted laser desorption/ionization time-of-flight/time-of-flight tandem mass spectrometry of carbohydrates. Rapid Commun. Mass Spectrom. **18**(4), 392–98 (2004)
44. Morelle, W., Slomianny, M.C., Diemer, H., Schaeffer, C., Dorsselaer, A.V., Michalski, J.C.: Fragmentation characteristics of permethylated oligosaccharides using a matrix-assisted laser desorption/ionization two-stage time-of-flight (TOF/TOF) tandem mass spectrometer. Rapid Commun. Mass Spectrom. **18**(22), 2637–49 (2004)
45. Stephens, E., Maslen, S.L., Green, L.G., Williams, D.H.: Fragmentation characteristics of neutral N-linked glycans using a MALDI-TOF/TOF tandem mass spectrometer. Anal. Chem. **76**(8), 2343–54 (2004)
46. Guerardel, Y., Chang, L.Y., Maes, E., Huang, C.J., Khoo, K.H.: Glycomic survey mapping of zebrafish identifies unique sialylation pattern. Glycobiology, in press (2006)
47. Ciucanu, I., Kerek, F.: A simple and rapid method for the permethylation of carbohydrates. Carbohydr Res. **131**(2), 209–17 (1984)
48. Dell, A., Reason, A.J., Khoo, K.H., Panico, M., McDowell, R.A., Morris, H.R.: Mass spectrometry of carbohydrate-containing biopolymers. Methods Enzymol. **230**, 108–32 (1994)
49. Domon, B., Costello, C.E.: A systematic nomenclature for carbohydrate fragmentations in FAB-MS/MS spectra of glycoconjugates. Glycoconj J. **5**, 397–409 (1988)
50. Harvey, D.J.: Structural determination of N-linked glycans by matrix-assisted laser desorption/ionization and electrospray ionization mass spectrometry. Proteomics **5**(7), 1774–86 (2005)
51. Cumming, D.A., Hellerqvist, C.G., Harris-Brandts, M., Michnick, S.W., Carver, J.P., Bendiak, B.: Structures of asparagine-linked oligosaccharides of the glycoprotein fetuin having sialic acid linked to N-acetylglucosamine. Biochemistry **28**(15), 6500–12 (1989)
52. Townsend, R.R., Hardy, M.R., Cumming, D.A., Carver, J.P., Bendiak, B.: Separation of branched sialylated oligosaccharides using high-pH anion-exchange chromatography with pulsed amperometric detection. Anal. Biochem. **182**(1), 1–8 (1989)
53. Taguchi, T., Seko, A., Kitajima, K., Muto, Y., Inoue, S., Khoo, K.H., Morris, H.R., Dell, A., Inoue, Y.: Structural studies of a novel type of pentaantennary large glycan unit in the fertilization-associated carbohydrate-rich glycopeptide isolated from the fertilized eggs of *Oryzias latipes*. J. Biol. Chem. **269**(12), 8762–71 (1994)